

SPECTRUM-LOADING FATIGUE-CRACK GROWTH  
FOR A SHIP STEEL IN SALTWATER\*

Yi-Wen Cheng  
Fracture and Deformation Division  
National Bureau of Standards  
Boulder, Colorado 80303

Keywords: corrosion fatigue; fatigue crack growth; fracture mechanics;  
seawater environment; spectrum loading; structural steel.

\*Contribution of NBS; not subject to copyright.

*International Journal of Fatigue, London, England.*

## ABSTRACT

Fatigue crack growth under spectrum loading intended to simulate sea-loading of offshore structures in the North Sea was studied using the fracture mechanics approach. A digital simulation technique was used to generate samples of load-time histories from a power spectrum characteristic of the North Sea environments. In the constant-load-amplitude tests, the effects of specimen orientation and stress ratio on fatigue crack growth rates were found to be negligible. Fatigue crack growth rates in a 3.5 percent NaCl solution were two to five times faster than those observed in air in the stress intensity range 25 to 60 MPa $\sqrt{\text{m}}$ . The average fatigue crack growth rates under spectrum loading and under constant-amplitude loading were in excellent agreement when fatigue crack growth rate was plotted as a function of the appropriately defined equivalent-stress-intensity range.

## INTRODUCTION

In recent years the petroleum industry has built offshore drilling and production platforms in deeper waters and more hostile climates. As the offshore platforms encounter more severe weather and rougher sea-state conditions, fatigue becomes a more important factor in consideration of structural integrity. In treating the fatigue problem, it is usual to separate the fatigue life into two separate stages: (1) crack initiation; and (2) crack growth. For welded structures, such as offshore platforms, crack initiation, during which microcracks form, grow, and coalesce to become a macrocrack, is less important because fabrication imperfections are always present. The majority of the fatigue life is spent in the crack growth stage.

Analysis of fatigue crack growth under spectrum loading, which is usually irregular in nature, is complicated because of load-sequence interaction effects. A cycle-by-cycle approach, taking into account overload effects, has been used in the aerospace industry [1,2]. Other empirical approaches, such as root mean square (RMS) [3] or root mean cube (RMC) [4], were also successfully used to correlate experimental results of spectrum loading of bridges with those of constant-amplitude loading. Use of the latter approaches is empirical and implementation of the former is time-consuming. A more efficient approach has been proposed [5,6], which will be discussed later. This paper describes work carried out at the National Bureau of Standards over the past two years on the investigation of fatigue crack growth in ABS grade EH36 steel under simulated offshore platform service conditions.

## LOAD SPECTRUM

Service loads acting on offshore structures are random in nature. The main source of cyclic loading derives from wave action which excites a vibration at approximately the wave frequency. The magnitude of the vibration depends mainly on wave height and direction, size of component and its location in a structure. Besides vibration due to wave action, additional vibrations are induced from structural responses to the wave action. The magnitude and frequency of the structural resonance depend on local structural characteristics. Thus, the precise definition of load-time history is extremely complex and would be expected to vary between different locations on the same structure.

Because of complexity in and lack of information on the precise load-time history experienced by offshore structures, no standard load-time history is available (or exists) for purposes of analysis and experiment. Numerous load-time histories, including Rayleigh peak distribution [7,8], Gaussian peak distribution [7-9], Gassner blocked program [10], and others [11], have been used to evaluate fatigue performance of weldments. The load spectrum selected for the present investigation was realistic for offshore structures in North Sea environments [12], as shown in Figure 1. The principal loads in this spectrum, those with a frequency of about 0.1 Hz, are due to wave action. The higher frequency (about 0.35 Hz) loads are due to the structural resonance.

## SIMULATION OF LOAD-TIME HISTORIES

For purpose of experiment, the power spectral density function,  $S(\omega)$ , is not sufficient; load-time history,  $X(t)$ , has to be used. In this investigation, the following expression [13,14] was used to reconstruct  $X(t)$  from  $S(\omega)$ :

$$X(t) = \sum_{k=1}^J [2G(\omega_k)\Delta\omega_k]^{\frac{1}{2}} \cos(\omega_k t + \phi_k) \quad (1)$$

where  $G(\omega)$ , as shown in Figure 1, is the one-sided power spectral density function in terms of frequency,  $\omega$  ( $G(\omega) = 2S(\omega)$  for  $\omega > 0$ ). Frequency is defined over the interval  $[0, \omega_u]$  with partitions of length such that

$$\omega_u = \sum_{k=1}^J \Delta\omega_k \quad (2)$$

$\phi$  is a random phase angle uniformly distributed between 0 and  $2\pi$ .  $\omega_k$  is the midpoint of  $\Delta\omega_k$ . The number of harmonic functions,  $J$ , is arbitrary; in this investigation it was taken to be 50.

An undesired periodic  $X(t)$  with a short period occurs if the minimum common divider for all the  $\omega_k$  is large. This problem is avoided by using random intervals for  $\Delta\omega_k$ . In this investigation,  $\Delta\omega_k$  was taken from a normal distribution with a mean equal to the average of  $\Delta\omega_k$  and a standard deviation equal to one-tenth of the average of  $\Delta\omega_k$ .

A computer program written in Fortran IV has been developed to simulate  $X(t)$  using Eq. (1). Newton's method was then used to locate peaks and troughs with respect to time in the simulated load-time history.

Two load spectra were used in this study. One considers only the wave-loading portion of the power spectral density function with frequency up to 0.2 Hz (Case I) as shown in Figure 1. The other considers the whole curve (Case II). Typical simulated load-time histories  $X(t)$ , from the power spectral density function are shown in Figure 2a and b.

Values of the irregularity factor (number of mean crossings/number of peaks plus troughs) calculated from the power spectra are 0.90 and 0.69 for Case I and Case II, respectively; they are 0.90 and 0.68, as determined from

the simulated load-time histories. The excellent agreement between the values obtained from the power spectra and the simulated load-time histories indicates that use of Eq. (1) is satisfactory. Values of the clipping ratio are 3.84 and 3.91 for Case I and Case II, respectively. Clipping ratio is defined as the ratio of the maximum load amplitude, which is the difference between the maximum peak and the mean load, to the root-mean-square value of load amplitude.

#### EXPERIMENTAL PROCEDURES

Test Material and Specimens: The test material was a 25.4-mm thick plate of ABS grade EH36 steel, a 350-MPa-yield-strength C-Mn steel. The chemical composition is given in Table 1. The steel was in the normalized condition and had particularly uniform properties due to sulfide shape control.

Fatigue crack growth rate (FCGR) tests under constant-amplitude loading and spectrum loading were conducted using standard (25.4-mm thick) and modified [15] compact specimens. The modified compact specimen was a lengthened and side-grooved (with a net thickness of 3.18 mm) version of the standard compact specimen. The deep side grooves determine the plane of crack growth and provide a strip of material that undergoes large cyclic plasticity during fatigue. Specimens were in LT and TL orientations.

Test Apparatus and Environment: Fatigue crack growth rate tests were conducted with a fully automated test system, which was described in a previous paper [16]. Briefly, the fully automated test system consists of a closed-loop, servo-controlled, hydraulic mechanical test machine, a programmable digital oscilloscope serving as an analog-to-digital converter, a programmable arbitrary waveform generator, and a minicomputer.

Tests were performed in laboratory air and in 3.5 percent NaCl solution with a free corroding condition (no cathodic protection). Crack lengths were

5

measured by the compliance technique. In the saltwater tests, the clip-gage used for displacement measurements was mounted on a scissors-like extension to avoid immersion in the saltwater. The environmental chamber was a 19-l-capacity plastic container. The saltwater is continuously circulated at a rate of 26 l/minute through a diatomaceous-earth filter. The NaCl concentration, temperature, and pH value of the saltwater was monitored periodically.

Loading Conditions: In the constant-load-amplitude tests, the stress ratio,  $R$ , that is the ratio of minimum to maximum stress, was kept constant at 0.1 or 0.5. Tests in air were conducted at 10 Hz and tests in 3.5 percent NaCl solution were conducted at 0.1 Hz. A sinusoidal load-time history was used.

In the spectrum-loading tests, the simulated load-time histories were recorded on floppy disks, which were read by a minicomputer. No modifications, such as truncation, on the simulated load-time histories were done, except on the levels of mean loads. The mean loads were increased so that the minimum loads were slightly above zero. This was done because the apparatus was limited to tension-tension loading. The stress ratio, therefore, varied from about 0 (usually for large load ranges) to about 1 (usually for very small load ranges).

Because of the limited capacity of the floppy disk, the total recorded lengths of load-time histories were 18.0 hours for Case I and 9.3 hours for Case II. The recorded lengths correspond to return periods of 15,773 and 11,890 mean-load crossings for Case I and Case II, respectively. The wave shape was triangular. It has been shown [17] that there are no differences in FCGR between tests conducted with sinusoidal and triangular waveforms. Both tests in air and in saltwater were conducted at ambient temperature.

## EXPERIMENTAL RESULTS AND DISCUSSION

Constant-Load-Amplitude Tests: Fatigue crack growth rates were calculated using the linear-elastic fracture mechanics approach; the experimental results are shown in Figures 3-6. As shown in Figure 3, specimen orientation, TL vs LT, had little influence on FCGR in air and in saltwater. The FCGR in air and in saltwater are compared in Figures 4 and 5. For stress intensity range,  $\Delta K$ , between 30 and 40 MPa $\sqrt{m}$ , the growth rates in saltwater were up to five times faster than those in air. A summary of all results, Figure 6, indicated that stress ratio had small influence on FCGR in air. Below  $4 \times 10^{-5}$  mm/cycle the FCGR in air and in saltwater were about the same.

Note that in each of the FCGR curves the high growth rate data were obtained with the modified compact specimen. The data obtained with the modified compact specimen follow the same trend line as the data obtained with the standard compact specimen. Thus it appears that the linear-elastic fracture mechanics approach can be applied to fatigue crack growth in conditions of contained large cyclic plasticity.

Spectrum Loading Tests: Fatigue crack growth rates under spectrum loading were analyzed using the equivalent-stress-range approach [5,6], which is described in the following. For simplicity the Paris equation,  $da/dN = C(\Delta K)^n$ , is used for discussion. Here,  $da/dN$  is crack growth increment per load cycle,  $\Delta K$  is stress intensity range, and  $C$  and  $n$  are constants.  $\Delta K$  is defined as

$$\Delta K = h (\pi a)^{\frac{1}{2}} Y \quad (3)$$

where  $h$  = stress range

$a$  = crack length

$Y$  = geometry factor

If  $da/dN \ll$  crack length,  $a$ , and there are no load-sequence interaction effects, then

$$\Delta a_1 = C h_1^n [(\pi a)^{1/2} Y]^n \quad (4)$$

$$\Delta a_2 = C h_2^n [(\pi a)^{1/2} Y]^n \quad (5)$$

...

...

...

$$\Delta a_N = C h_N^n [(\pi a)^{1/2} Y]^n \quad (6)$$

Summing Eqs. (4) through (6) gives

$$(\Delta a_1 + \Delta a_2 + \dots + \Delta a_N) = C (h_1^n + h_2^n + \dots + h_N^n) [(\pi a)^{1/2} Y]^n \quad (7)$$

The left-hand side of Eq. (7) is the increment of crack growth in N successive cycles; the average FCGR per cycle is then

$$da/dN = C [(h_1^n + h_2^n + \dots + h_N^n)/N] [(\pi a)^{1/2} Y]^n \quad (8)$$

$$= C [(\overline{h^n})^{1/n} (\pi a)^{1/2} Y]^n \quad (9)$$

$$= C [h_{eq} (\pi a)^{1/2} Y]^n$$

Here N should be large in order for the equivalent-stress-range,  $h_{eq}$ , to be representative of a load spectrum. The definitions of stress range and cycle used in this investigation are given in Figure 7. The value of n in 3.5 percent NaCl solution test is 5.5, which is derived from the results of constant-load-amplitude test in the  $\Delta K$  range of interest.

The results for FCGR under spectrum loading in 3.5 percent NaCl solution are given in Figures 8 and 9 for Case I and Case II, respectively. Excellent agreement between spectrum and sinusoidal loading is observed. This suggests that load-sequence interaction effects are effectively negligible. The results also imply that at a given  $\Delta K$  value, use of RMS (n=2) or RMC (n=3)

approach will predict faster FCGR in spectrum loading than in sinusoidal loading because  $h_{eq}$  increases with  $n$ .

Miner's rule [18] states that a component (or specimen) will fail if

$$\sum (f_i / F_{if}) \geq 1 \quad (10)$$

where  $f_i$  = number of fatigue cycles applied at stress range  $\Delta S_i$

$F_{if}$  = number of fatigue cycles to failure at stress range  $\Delta S_i$

This rule implies that there are no load-sequence interaction effects. Miner's rule, as originally stated, applied to fatigue failure rather than fatigue crack growth. Terms such as "Miner's rule fatigue crack growth" are often used to mean fatigue crack growth with no load-sequence interaction effects. Such statements represent a generalization of the original Miner's rule. The data of this study along with others [5] support such a generalization for clipping ratio less than 4 and constant mean stress, which might be stated as follows: Load-sequence interactions are small, or they tend to cancel, such that the overall effect on fatigue life is small. In order for such a rule to be applicable to random or quasi-random load-time histories, a definition of a cycle is needed. In this study, the load amplitude of one cycle has been defined as the maximum load difference among three successive mean-crossings (Figure 7).

The value of  $h_{eq}$  can be obtained in a closed-form expression from the power spectrum if the loading is a narrow-band random process [6,19].

However, no closed-form solutions are available for wide-band random processes.

## CONCLUSIONS

The following conclusions were drawn from this investigation:

1. The digital simulation technique is adequate to generate samples of load-time histories from a given power spectrum.
2. In constant-load-amplitude tests, the influence of specimen orientation and stress ratio on fatigue crack growth rate were found to be negligible. Fatigue crack growth rates in a 3.5 percent NaCl solution were two to five times faster than those observed in air in the stress intensity range 25 to 60 MPa $\sqrt{m}$ .
3. The average fatigue crack growth rates under spectrum loading and under constant-amplitude loading were in excellent agreement when fatigue crack growth rate was plotted as a function of the appropriately defined equivalent-stress-intensity range. This procedure is equivalent to applying Miner's summation rule in fatigue life calculations.

## ACKNOWLEDGMENTS

Helpful discussions with Drs. H. I. McHenry, and D. T. Read, and Professors S. Berge and P. N. Li are appreciated. This work is supported by the Department of Interior, Minerals Management Service.

## REFERENCES

1. O. E. Wheeler, "Spectrum Loading and Crack Growth," J. of Basic Engineering, Trans. ASME, Vol. 94, (March 1972), pp. 181-186.
2. J. Willenborg, R. M. Engle, and H. A. Wood, "A Crack Growth Retardation Model Using An Effective Stress Concept," AFFDL-TM-71-FBR, Air Force Flight Dynamics Laboratory, Dayton, Ohio, January 1971.
3. J. M. Barsom, "Fatigue Crack Growth Under Variable-Amplitude Loading in Various Bridge Steels," in: Fatigue Crack Growth Under Spectrum Loads, ASTM STP 595, American Society for Testing and Materials, Philadelphia (1976), pp. 217-235.
4. P. Albrecht and K. Yamada, "Simulation of Service Fatigue Loads for Short-Span Highway Bridges," in: Service Fatigue Loads Monitoring, Simulation, and Analysis, ASTM STP 671, American Society for Testing and Materials, Philadelphia (1979), pp. 255-277.
5. W. D. Dover, S. J. Holbrook, and R. D. Hibberd, "Fatigue Life Estimates for Tubular Welded T Joints Using Fracture Mechanics," in: Proceedings of European Offshore Steels Research Seminar, The Welding Institute, Cambridge, UK, November 27-29, 1978, pp. V/PD-1 - V/PD-11.
6. F. A. McKee and J. W. Hancock, "Fatigue Crack Growth and Failure in Spectrum Loading," *ibid.*, pp. V/PC-1 - V/PC-10.
7. L. P. Pook, "Proposed Standard Load Histories for Fatigue Testing Relevant to Offshore Structures," NEL Report No. 624, National Engineering Laboratory, Glasgow, UK, October 1976.
8. M. H. J. M. Zwaans, P. A. M. Jonkers, and J. L. Overbeeke, "Random Load Tests on Plate Specimens," Eindhoven University of Technology, the Netherlands, December 1980.

- 11
9. P. J. Haagenzen and V. Dagestad, "Corrosion Fatigue Crack Propagation in Structural Steel under Stationary Random Loading," SINTEF Report No. 18 A 78017, The Foundation of Scientific and Industrial Research at the Norwegian Institute of Technology, Norway, October 2, 1978.
  10. H. P. Lieurade, J. P. Gerald, and C. J. Putot, "Fatigue Life Prediction of Tubular Joints," Proceedings of the Offshore Technology Conference, OTC Paper No. 3699, Houston, Texas, May 1980.
  11. R. M. Olivier, M. Greif, W. Oberparleiter, and W. Schutz, "Corrosion Fatigue Behavior of Offshore Steel Structures under Variable Amplitude Loading," Proceedings of International Conference on Steel in Marine Structures, Paper 7.1, Paris, France, October 5-8, 1981.
  12. R. M. Kenley, "Measurement of Fatigue Performance of Forties Bravo," Proceedings of the Offshore Technology Conference, OTC Paper No. 4402, May, 1982.
  13. J.-N. Yang, "Simulation of Random Envelop Processes," J. of Sound and Vibration, Vol. 21, No. 1, (1972), pp. 73-85.
  14. P. H. Wirsching and A. M. Shehata, "Fatigue under Wide Band Random Stresses Using the Rain-Flow Method," J. of Engineering Materials and Technology, Trans. ASME, Vol. 99, No. 3, (July 1977), pp. 205-211.
  15. H. I. McHenry and G. R. Irwin, "A Plastic-Strip Specimen for Fatigue Crack Propagation Studies in Low Yield Strength Alloys," J. of Materials, JMLSA, Vol. 7, No. 4, (December 1972), pp. 455-459.
  16. Y. W. Cheng and D. T. Read, "An Automated Fatigue Crack Growth Rate Test System," to be published in the Proceedings of Symposium on Automated Test Methods for Fracture and Fatigue Crack Growth, November 7-8, 1983, Pittsburgh, Pennsylvania.

17. J. M. Barsom, "Effect of Cyclic Stress Form on Corrosion Fatigue Crack Propagation Below  $K_{Isc}$  in a High Yield Strength Steel," in: Corrosion Fatigue: Chemistry, Mechanics, and Microstructure, National Association for Corrosion Engineers, NACE-2, (1972), pp. 424-435.
18. M. A. Miner, "Cumulative Damage in Fatigue," J. of Applied Mechanics, Trans. ASME, Vol. 12, (Sept. 1945), pp. A159-A164.
19. J.-N. Yang, "Statistics of Random Loading Relevant to Fatigue," J. of the Engineering Mechanics Division, Proceedings of the American Society of Civil Engineers, Vol. 100, No. EM3, (June 1974), pp. 469-475.

## List of Tables

1. Chemical composition of ABS grade EH36 steel.

## List of Figures

1. Characteristic power spectrum of offshore structures in the North Sea.
2. Samples of load-time histories: (a) Case I (b) Case II.
3. Fatigue crack growth rates in EH36 steel: effect of specimen orientation.
4. Fatigue crack growth rates in EH36 steel: saltwater vs air at stress ratio equal to 0.1.
5. Fatigue crack growth rates in EH36 steel: saltwater vs air at stress ratio equal to 0.5.
6. Fatigue crack growth rates in EH36 steel: summary.
7. Definitions of stress range and cycle.
8. Fatigue crack growth rates in EH36 steel in saltwater: constant-amplitude loading vs spectrum loading (Case I).
9. Fatigue crack growth rates in EH36 steel in saltwater: constant-amplitude loading vs spectrum loading (Case II).

Table 1. Chemical Composition of ABS Grade EH36 Steel

C	Mn	P	S	Si	Cu	Ni	Cr	Mo	Fe
0.12	1.39	0.015	0.006	0.380	0.05	0.03	0.05	0.007	bal.

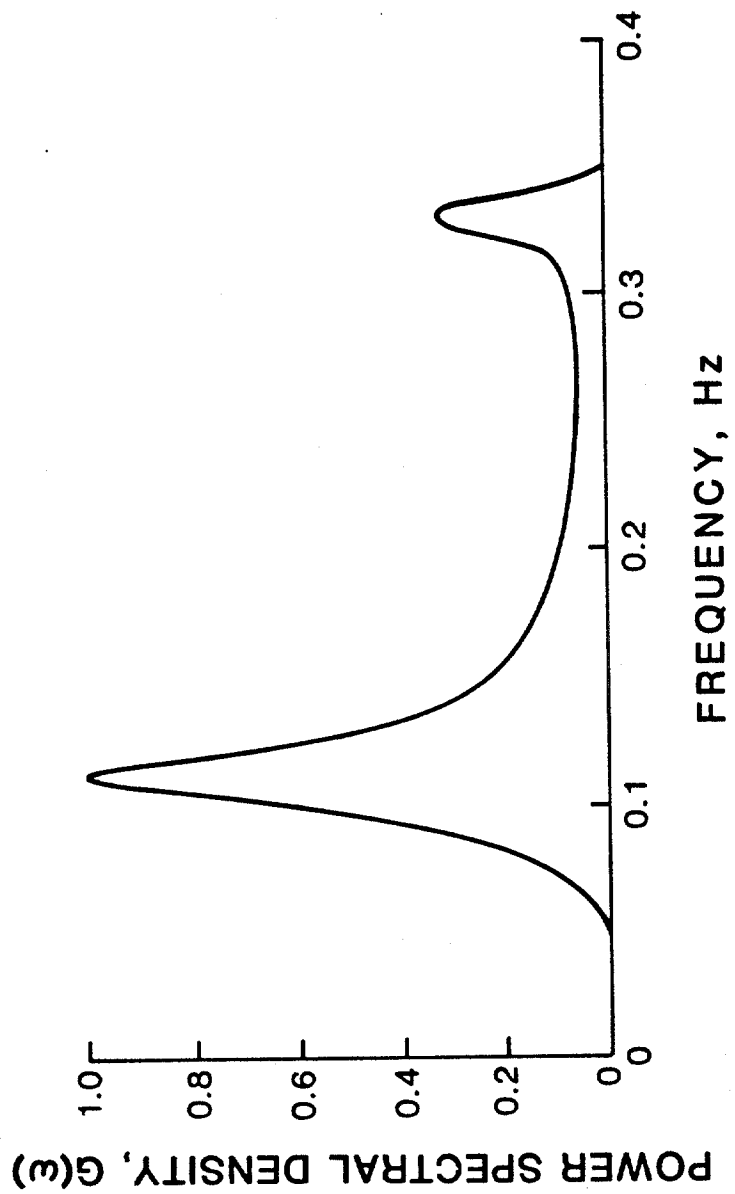
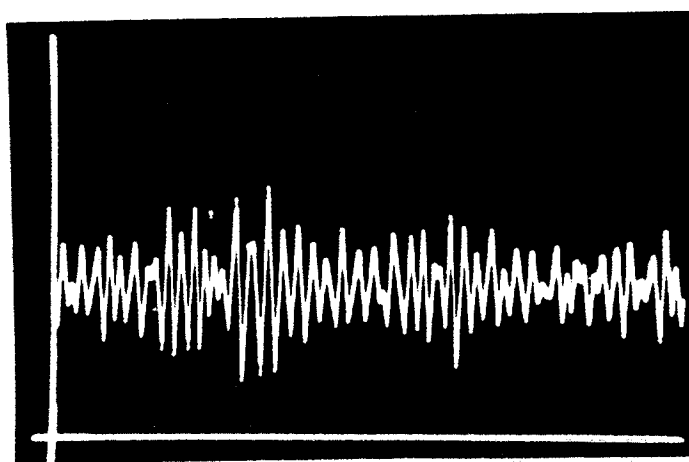
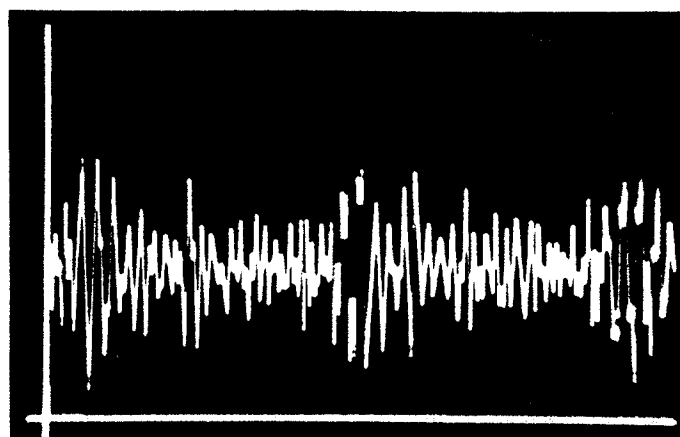


Fig 1



5 min.

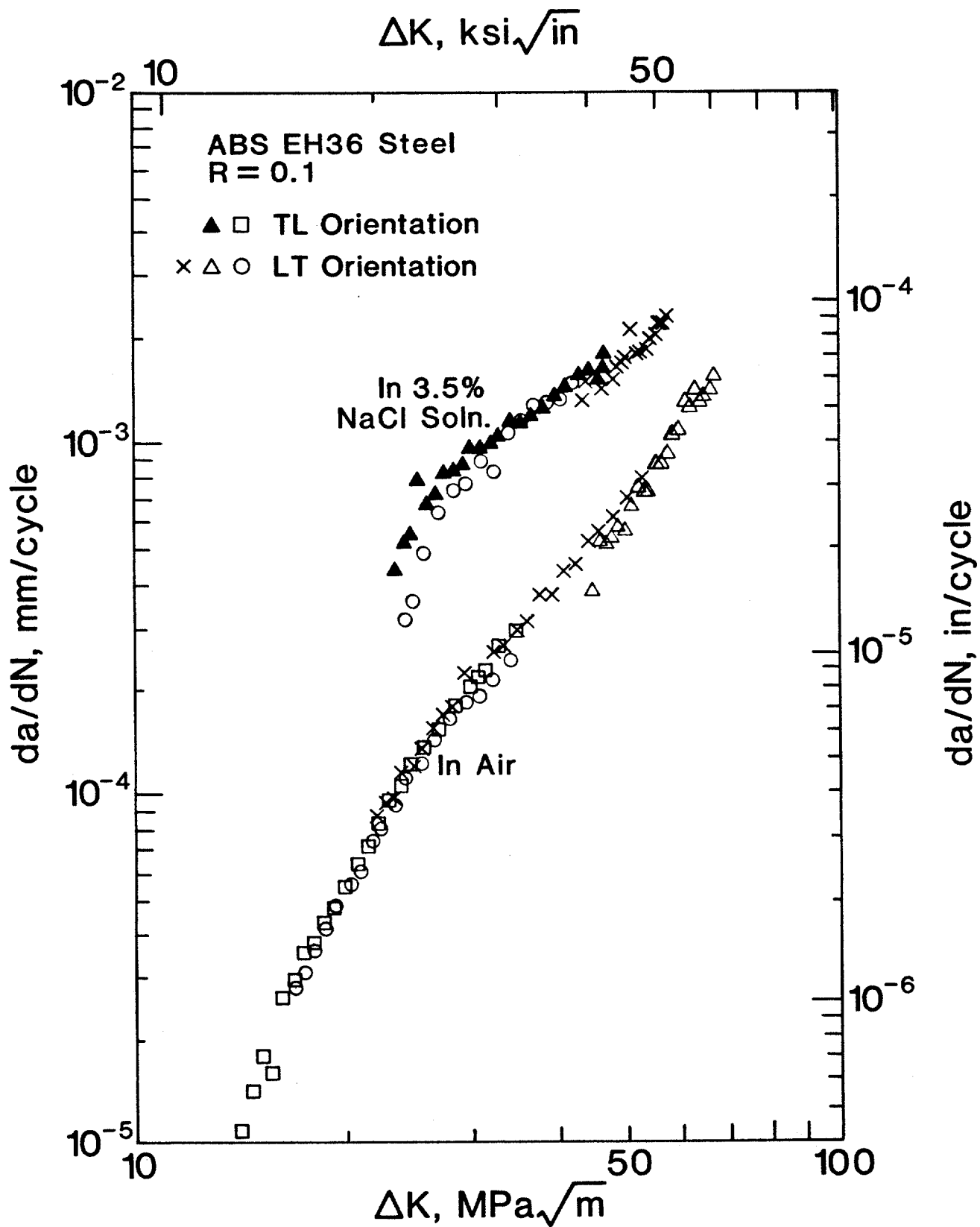
(a)

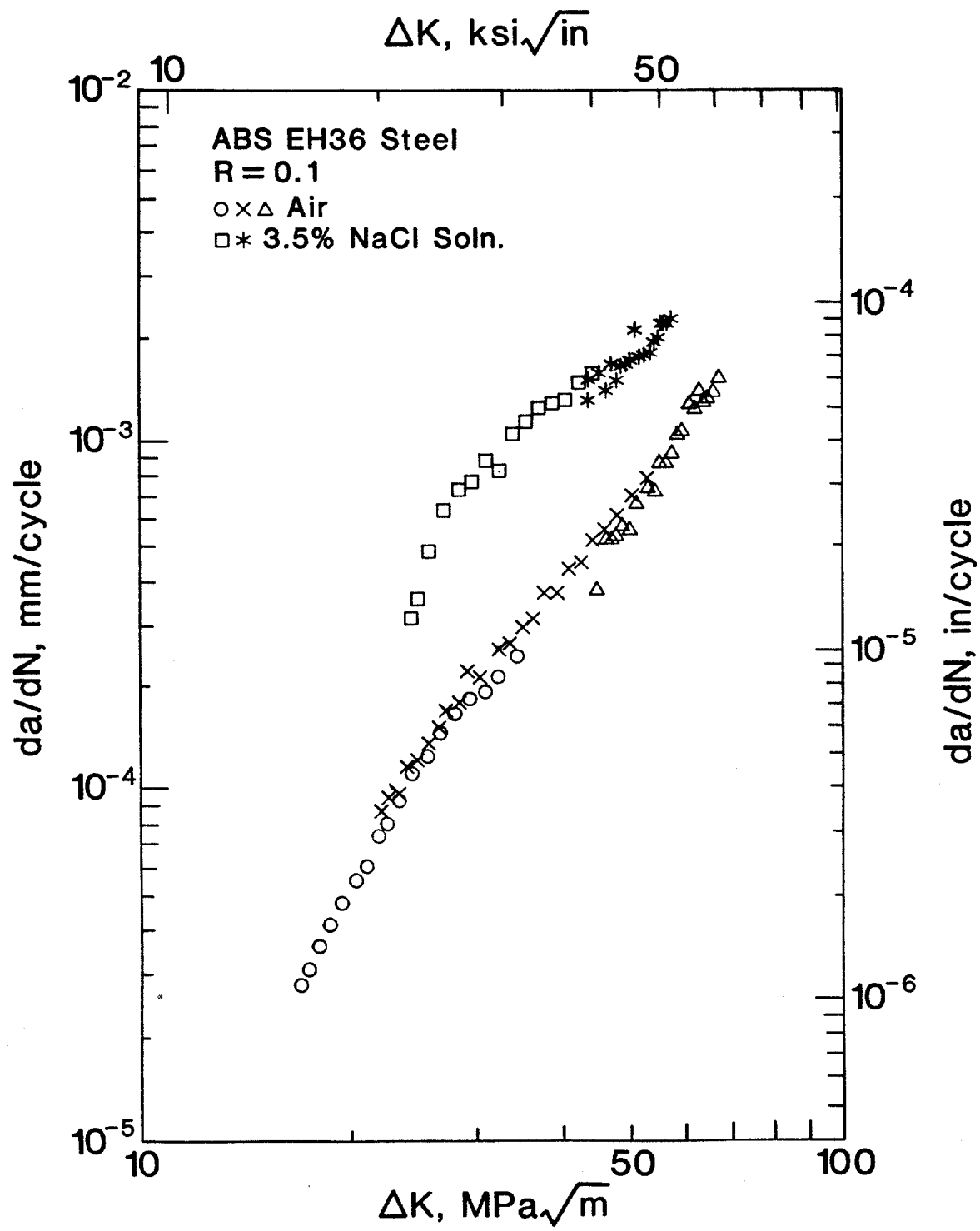


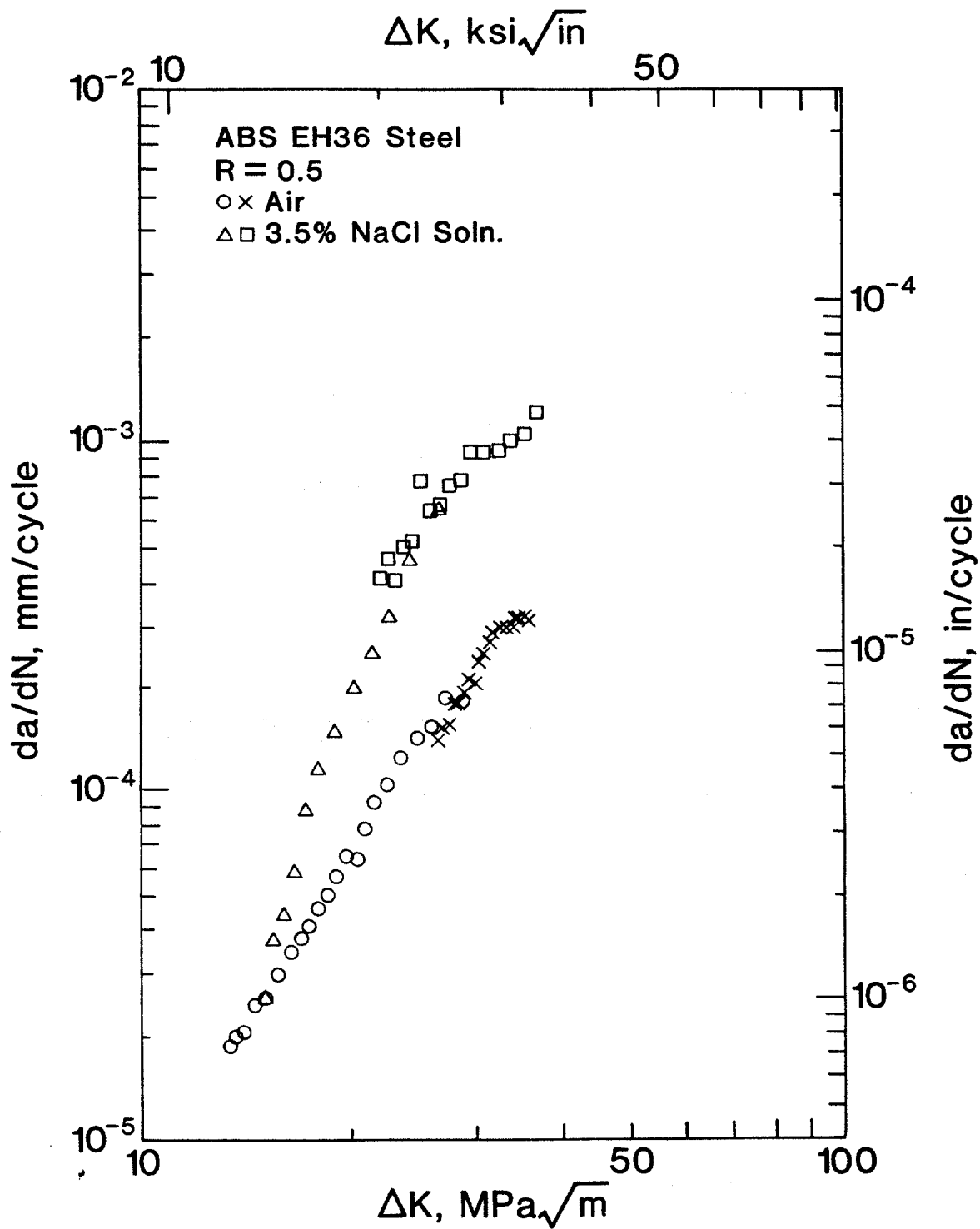
5 min.

(b)

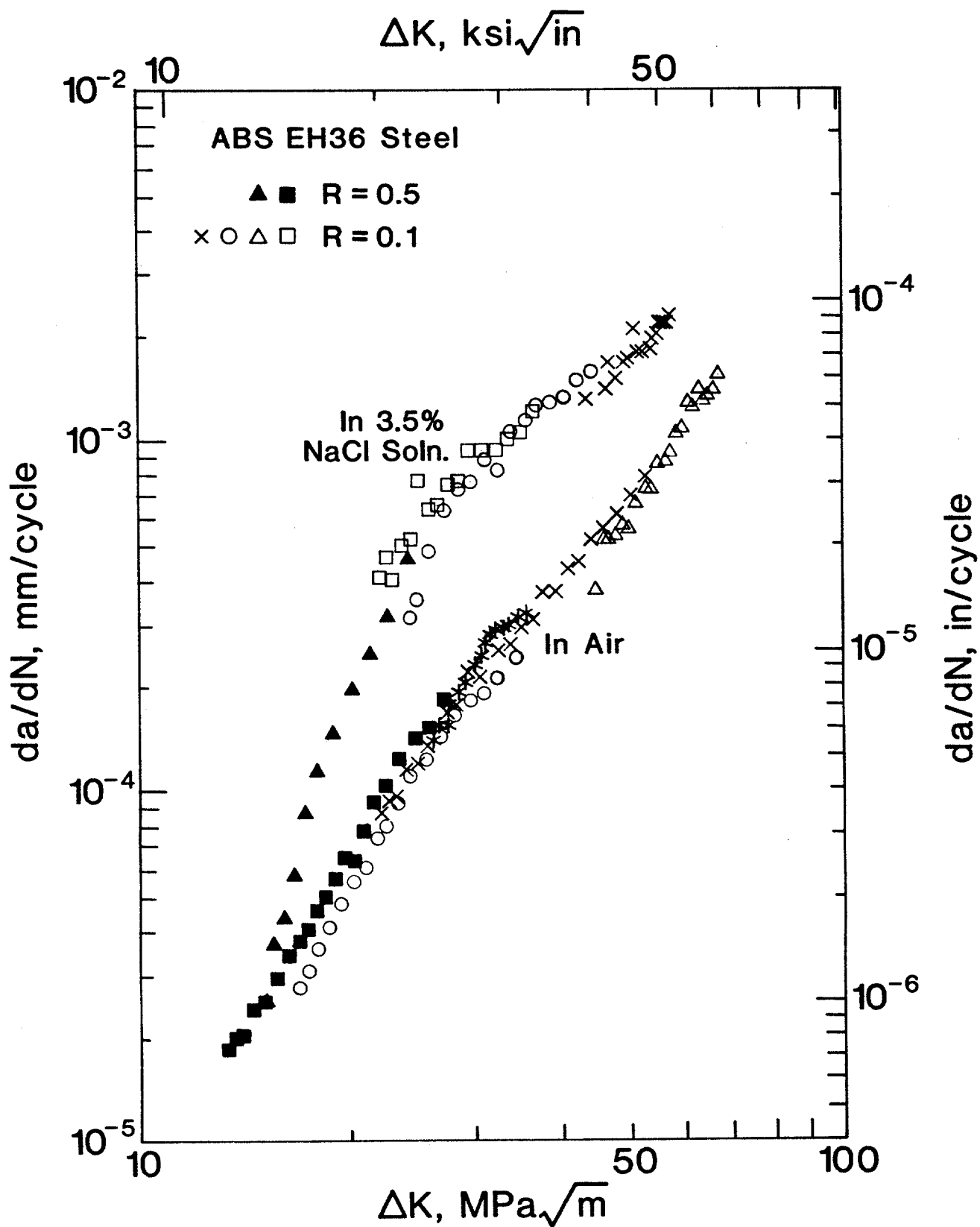
fig. 2







2-85



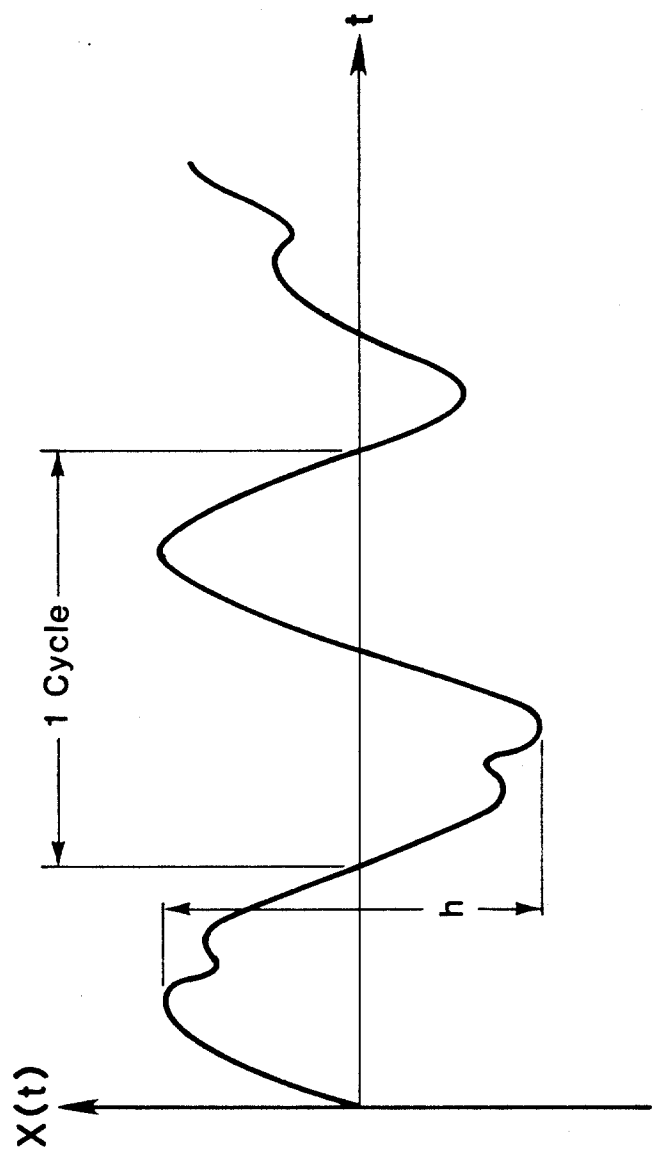


Fig. 7

